

# Monitoring the Shape Evolution of Silver Nanoplates: A Marker Study\*\*

James Goebel, Qiao Zhang, Le He, and Yadong Yin\*

In the past two decades, substantial efforts have been made to control the shape of nanostructured materials because of their strong shape-dependent chemical and physical properties. Classic examples include semiconductor nanorods that exhibit linearly polarized emission<sup>[1]</sup> and metal nanoplates that show tunable surface plasmon resonance.<sup>[2]</sup> To study the mechanism of shape evolution during nanostructure growth, aliquots are often removed from a reacting solution and the particles are analyzed using imaging techniques, such as transmission electron microscopy (TEM). However, as it is impossible to continuously monitor the growth of one particular particle, this catch-and-see method may not be able to unambiguously reveal the exact growth mechanism. One example is an interesting triangle-round-hexagon-triangle shape transition that we have recently observed during the seeded growth of silver nanoplates.<sup>[3]</sup> This transition has been very difficult to explain based on the simple observation of the shape change. Herein we demonstrate that the marker technique, which was widely used in studying atomic diffusion phenomena,<sup>[4]</sup> can be successfully adopted to help outline the original boundaries of the silver nanoplate, provide a clear picture of plate growth, and give insight into possible structures for the original seed and final product.

Colloidal silver nanoplates have been intensively studied due to their exceptional plasmonic properties and the related applications.<sup>[5]</sup> They can be synthesized using either photo-induced<sup>[2,6]</sup> or chemical reduction of  $\text{Ag}^+$  in the presence<sup>[7]</sup> or absence of seeds,<sup>[8]</sup> each of which produces uniform triangular nanoplates with relatively high yield. Further research has investigated ways to alter the morphology of nanoplates using either chemical<sup>[9]</sup> or photomediated etching,<sup>[10]</sup> which enables precise control over the optical properties. We and other groups have also explored seeded growth processes for synthesizing larger nanoplates with very high aspect ratios.<sup>[3,11]</sup> In addition, the study of their structure and the

mechanism which induces this structure has also received much attention.<sup>[12]</sup> It is generally understood that the plates are fcc crystals containing single {111} facets on their two planar surfaces.<sup>[13]</sup> The facet composition of the nanoplate sides is less clear, although recent high-resolution TEM experiments indicate a mixture of {100} and {111} facets.<sup>[14]</sup> Forbidden reflections of  $1/3\{422\}$  are observed, which are attributed to internal stacking faults parallel to the nanoplate surface. While the effects of surfactants and other synthetic conditions are significant, these defects are believed to be the driving factor behind the two-dimensional anisotropic growth.<sup>[15]</sup>

Recently, we reported a procedure for the synthesis of large Ag nanoplates using previously synthesized smaller plates as seeds.<sup>[3]</sup> When  $\text{Ag}^+$  was added to silver nanoplate seeds in the presence of reducing agent and citrate ions, the citrate selectively hindered growth on the {111} planar surface, allowing growth to occur only at the edges to produce high aspect ratio nanoplates. We observed in the early stages of  $\text{Ag}^+$  addition that the plates became largely circular, which was attributed to instability of the original seeds resulting from the removal of the stabilizing ligand PVP. However, when this synthesis is performed using more uniform triangular plates as seeds, for which washing is unnecessary due to modification of the seed synthesis to exclude PVP,<sup>[16]</sup> a notable shape transition from triangular to circular can still be observed, depicted in representative TEM images in Figure 1.

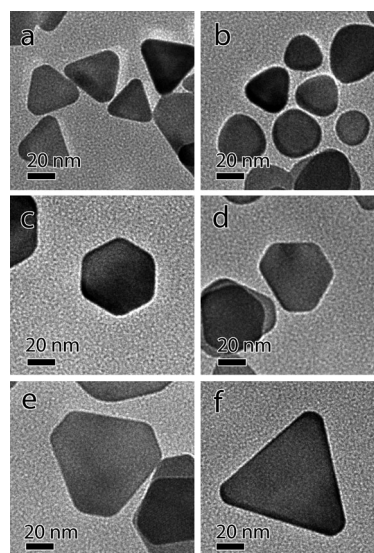


**Figure 1.** Step-by-step growth of large silver nanoplates using small plates as seeds. Images show a) the original sample and the sample after the addition of b) 0.3  $\mu\text{mol}$ , c) 2  $\mu\text{mol}$ , d) 3  $\mu\text{mol}$ , e) 4.5  $\mu\text{mol}$ , and f) 9.5  $\mu\text{mol}$  of silver nitrate.

[\*] J. Goebel, Q. Zhang, L. He, Prof. Y. Yin  
Department of Chemistry, University of California  
Riverside, CA 92521 (USA)  
E-mail: yadong.yin@ucr.edu  
Homepage: <http://faculty.ucr.edu/~yadong/>

[\*\*] We thank the U. S. National Science Foundation (DMR-0956081), and Department of Energy (DE-SC0002247) for support of this research. Y.Y. also thanks the Research Corporation for Science Advancement for the Cottrell Scholar Award, 3M for the Nontenured Faculty Grant, and DuPont for the Young Professor Grant. We thank Dr. Bozhilov and Mr. McDaniel at the Central Facility for Advanced Microscopy and Microanalysis at UCR for assistance with TEM analysis.

Supporting information for this article is available on the WWW under <http://dx.doi.org/10.1002/anie.201107240>.

Initially, the nanoplate seeds are mostly triangular (Figure 1a), but after only a small amount of silver precursor is added to the solution the plates become noticeably more rounded (Figure 1b). With further  $\text{Ag}^+$  addition, the nanoplates become roughly hexagonal (Figure 1c), and finally return to their original triangular shape, albeit larger (Figure 1f). The shape transition is confirmed by plasmonic shifts in the corresponding extinction spectra (Figure 2). In the early stages of growth, the plasmon band blueshifts (Fig-

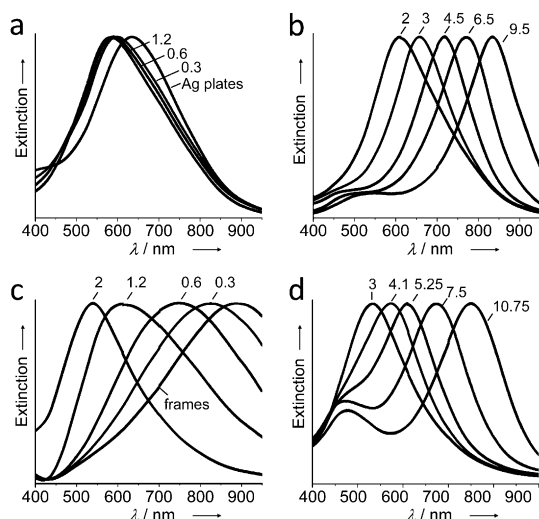


**Figure 2.** Normalized UV/Vis extinction spectra of samples after the addition of increasing amounts of silver nitrate: a) blueshift and b) subsequent redshift of Ag nanoplate-seeded sample during growth; c) blueshift and d) redshift of nanoframe-seeded sample during growth. The amount of  $\text{Ag}^+$  ion is shown on the corresponding spectrum in  $\mu\text{mol}$ .

ure 2a), which is indicative of the plates becoming more rounded as has been noted in the literature.<sup>[17]</sup> Later, the spectrum begins to redshift as a result of the plates growing laterally and is consistent with our prior observations concerning seeded nanoplate growth.

A similar shape transition has been reported in recent publications<sup>[11,18]</sup> and in one case was attributed to the possibility that a truncated structure might be more thermodynamically stable, but that the growth was kinetically controlled and thus ultimately the plates returned to their original triangular shapes. Although cursory examination of the step by step growth of the plates confirms that a shape change occurs, more in-depth study is necessary to fully comprehend its underlying causes and mechanism. To acquire a better understanding of this system, we have performed a straightforward but informative marker experiment using galvanic replacement by gold cations,<sup>[19]</sup> followed by seeded growth using the resulting nanoframe structure as a seed. Owing to the significant difference in atomic number between silver and gold and their small lattice mismatch, gold has suitable contrast with silver and can also readily seed the growth of silver,<sup>[20]</sup> making it a suitable choice of marker. By partially replacing the silver in the nanoplate with gold, we

can outline the original boundaries of the silver nanoplate, clarifying observations of subsequent seeded growth.

Interestingly, frames can act as seeds for large silver-plate growth in a nearly identical manner to that of normal small silver plates, depicted in TEM images in Figure 3. Upon the

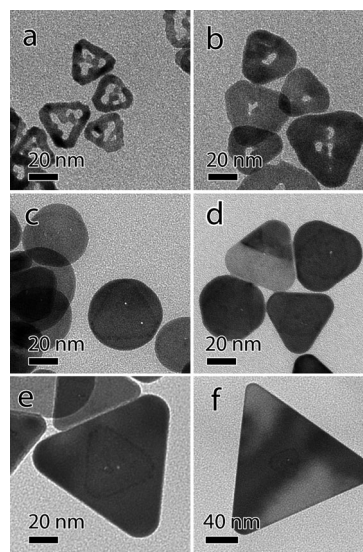


**Figure 3.** Step-by-step growth of silver nanoplates using Au nanoframes as seeds. a) Au nanoframe seeds and frame/plates after the addition of b) 0.3  $\mu\text{mol}$ , c) 3  $\mu\text{mol}$ , d) 4.1  $\mu\text{mol}$ , e) 7.5  $\mu\text{mol}$ , and f) 10.75  $\mu\text{mol}$  of silver nitrate.

addition of silver growth solution, the gold nanoframes are initially backfilled with silver (Figure 3b and c) and then undergo normal growth into large nanoplates (Figure 3d–f). Backfilling occurs first because of deposition at high-energy facets in the frame interior,<sup>[19]</sup> after which lateral outward growth proceeds. This assertion is supported by corresponding extinction spectra, which depict the initial blueshift (Figure 2c) and ensuing redshift (Figure 2d) of the in-plane dipole of the nanoframes, which are indicative of silver deposition and increasing aspect ratio, respectively.

The presence of gold frames as markers enables significant insights to be obtained from TEM observations during growth. After the initial backfilling step, the frame/plates grow outward in the same manner as silver nanoplates, undergoing a similar shape transition and ultimately returning to a triangular morphology (Figure 3d–f). Notably, throughout the various stages of outward growth, there is a preference for deposition on the edges of the frame/plates with little to none occurring at the corners, causing the triangular to circular/hexagonal transition. As more silver is deposited, the shape returns to triangular as a result of new corners being formed at the deposition sites (Figure 3e), resulting in a sample of frame/plates in which the majority contain an embedded frame pointed 180° relative to the orientation of the silver plate. Further silver addition results in the plate growing larger but does not induce additional shape changes (Figure 3f), which is consistent with our previous work.<sup>[3]</sup> These results indicate that the cause of the observed shape

transition is the almost exclusive deposition of silver on the nanoplate edges.

Clarification of the means of shape transition leads to the additional question of why the transition occurs in this manner. The fact that deposition occurs selectively and only one shape change takes place during growth implies that the original nanoplate seed structure changes to a more stable morphology over the course of the growth process. To explain the selective edge deposition, we employ a structural model proposed recently by Kelly and co-workers.<sup>[14]</sup> Based on HRTEM experiments, they ascertained that Ag nanoplates are comprised of two fcc regions of different thicknesses sandwiching an hcp layer originating from a series of internal stacking faults. To explain this observation, they devised a model in which each nanoplate edge consists of a {111} facet and a {100} facet of different sizes, which is possible due to the twinning in the center of the plate. Thus, a truncated triangular nanoplate should contain six edges, half featuring a larger {111} facet and half with a dominant {100} facet (Figure 4, center structure). This model suggests that the

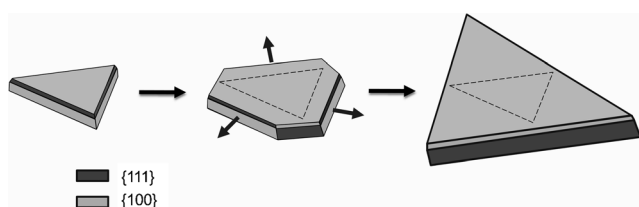


**Figure 4.** Schematic illustration of the structural change of Ag nanoplates during seeded growth. Preferential silver deposition on the {100} dominated edges of the seeds leads to a rounded or hexagonal intermediate with a mix of {100} and {111} dominated edges, after which further silver deposition produces a larger triangular plate with {111} dominated edges.

triangular shape of silver nanoplates is due to preferential deposition on the less thermodynamically stable {100} dominated edges, producing a triangular structure bounded by {111} dominated edges.

Using this model, the mechanism behind our observations can readily be explained, as illustrated in Figure 4. Initially, the sample consists of triangular nanoplates with {100} dominated edges. Although this is less thermodynamically stable than a {111} dominated configuration, it occurs because the rapid reduction by borohydride produces seeds under kinetic conditions, which favor {100} dominated edges. This assumption can also explain why other groups have had difficulty obtaining stable nanoplates without PVP or another {100} specific ligand.<sup>[8a]</sup> During subsequent seeded growth, ascorbic acid is used as the reducing agent and the  $\text{Ag}^+$  concentration is deliberately kept low, leading to a slower reaction rate, creating conditions in which thermodynamic considerations are of primary importance. As a result, a structure with the highest percentage of {111} surfaces is the most stable configuration, leading to selective deposition on {100} dominated sides and causing the observed shape transition to a structure with {111} dominated edges.

To further support this assertion, we performed an additional experiment in which seeded growth was performed in the presence of PVP and absence of citrate, as shown in Figure 5. While citrate primarily adheres to {111} surfaces,

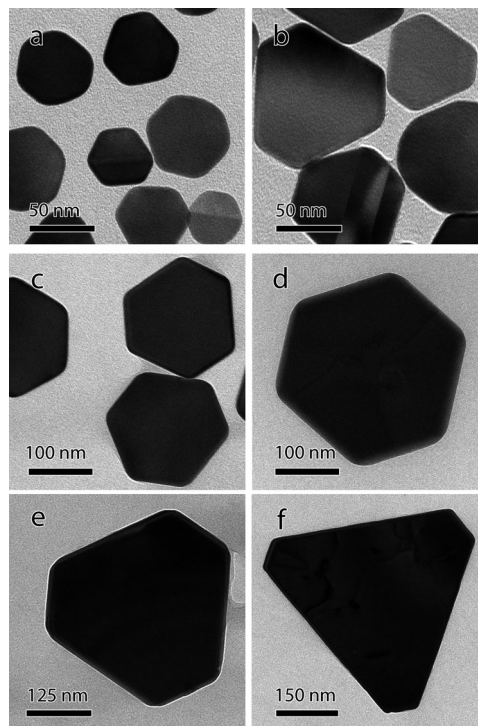


**Figure 5.** Stepwise growth of silver nanoplates with PVP present. Sample after the addition of a) 2.5  $\mu\text{mol}$ , b) 10  $\mu\text{mol}$ , c) 20  $\mu\text{mol}$ , d) 30  $\mu\text{mol}$ , e) 40  $\mu\text{mol}$ , and f) 50  $\mu\text{mol}$  of silver nitrate.

PVP selectively blocks growth on {100} surfaces and as such, should interfere with the lateral growth of the plates as well as the accompanying shape transition. Because of the lack of citrate in the system, growth on the planar surfaces of the nanoplates is more favorable and they become substantially thicker during the course of the reaction, evidenced by the greater contrast compared with citrate grown plates. Additionally, a triangular to hexagonal to triangular shape transition is still evident and the plates also grow laterally, indicating that in spite of the different surfactant system some deposition still occurs on the plate edges and the overall mechanism of growth is the same. These results are consistent with those obtained by Xia et al. from a similar synthesis.<sup>[11]</sup> Most significantly, however, is the fact that the shape transition is “delayed” in the sense that the PVP grown plates are much larger (ca. 530 nm edge length) than their citrate grown counterparts (ca. 90 nm edge length) at the point at which the growth transition is nearly complete. This observation implies the seeds have {100} dominated edges, because while a shape transition still occurs, it is effectively retarded by the selective {100} adhesion of PVP. The smaller energy difference between {111} and {100} surfaces enables substantial deposition at both the {100} and {111} surfaces on the plate edges, resulting in a “slower” shape transition due to the decreased preference for {100} deposition. These results



further support that the shape transition is motivated by the thermodynamically induced switch from a nanoplate with {100} dominated sides to a structure with {111} dominated edges.

In summary, we have presented a new marker technique which uses embedded Au frames as markers to define the original boundaries of small silver nanoplates utilized in a seeded growth reaction, clarifying the nature of an observed reversible shape change which takes place during growth. Based on the opposing orientations of the inner frame and surrounding plate, it is apparent that the shape transition is caused by the nanoplates morphing from structures with primarily {100} facets on their edges into more thermodynamically stable structures with {111} dominated edges through selective silver deposition on {100} facets. This transition would be very difficult to observe with conventional methods but with the addition of a gold marker it becomes readily apparent. We believe the marker technique might have the potential to become a general tool to help determine the mechanism of shape evolution of nanostructures.

### Experimental Section

**Seeded growth of silver nanoplates:** Nanoplate seeds are first synthesized using a modified chemical reduction method based on previous reports.<sup>[8a,16]</sup> Seeded growth is then performed using a technique developed in our group.<sup>[3]</sup> First, the as-synthesized seeds are collected by centrifugation for 14 min at 15000 rpm and then re-suspended in a solution comprising deionized H<sub>2</sub>O (20 mL), trisodium citrate (TSC) (75 mM, 250  $\mu$ L), and L-ascorbic acid (AA, 0.1M, 750  $\mu$ L). The nanoplate solution is stirred rapidly, after which growth is initiated by using a syringe pump to slowly add (0.2 mL/minute) silver growth solution, containing silver nitrate (1 mM, 40 mL), citric acid (0.1M, 250  $\mu$ L), and TSC (1.5 mM, 200  $\mu$ L).

**Nanoplate growth using gold frames as seeds:** Nanoplate seeds are centrifuged and collected in the manner described above, except they are suspended in a solution containing H<sub>2</sub>O (25 mL), TSC (30 mM, 1.5 mL), and PVP (29000 MW, 0.7 mM, 1.5 mL). The solution is then stirred rapidly and heated to 60°C, after which HAuCl<sub>4</sub> (1 mM, 800  $\mu$ L) is slowly added. The frames are collected by centrifugation for 14 min at 15000 rpm, and then re-suspended in a solution containing H<sub>2</sub>O (20 mL), TSC (75 mM, 250  $\mu$ L) and AA (0.1M, 750  $\mu$ L). Backfilling and growth is initiated by adding the same silver growth solution at the same rate used for the silver plate seeds by syringe pump, and ceases upon stopping the injection.

Received: October 13, 2011

Published online: November 29, 2011

**Keywords:** marker study · nanoplates · seeded growth · shape transition · silver

- [1] J. Hu, L.-s. Li, W. Yang, L. Manna, L.-w. Wang, A. P. Alivisatos, *Science* **2001**, 292, 2060–2063.
- [2] R. C. Jin, Y. C. Cao, E. C. Hao, G. S. Metraux, G. C. Schatz, C. A. Mirkin, *Nature* **2003**, 425, 487–490.
- [3] Q. Zhang, Y. X. Hu, S. R. Guo, J. Goebel, Y. D. Yin, *Nano Lett.* **2010**, 10, 5037–5042.
- [4] a) J. Baglin, F. d'Heurle, S. Peterson, *Appl. Phys. Lett.* **1978**, 33, 289; b) J. Lutz, J. K. N. Lindner, S. Mändl, *Appl. Surf. Sci.* **2008**, 255, 1107–1109; c) A. D. Smigelskas, E. O. Kirkendall, *Trans. AIME* **1947**, 171, 130–142.
- [5] a) R. C. Jin, Y. W. Cao, C. A. Mirkin, K. L. Kelly, G. C. Schatz, J. G. Zheng, *Science* **2001**, 294, 1901–1903; b) I. Pastoriza-Santos, L. M. Liz-Marzan, *J. Mater. Chem.* **2008**, 18, 1724–1737; c) I. Pastoriza-Santos, R. A. Alvarez-Puebla, L. M. Liz-Marzan, *Eur. J. Inorg. Chem.* **2010**, 4288–4297; d) J. An, B. Tang, X. L. Zheng, J. Zhou, F. X. Dong, S. P. Xu, Y. Wang, B. Zhao, W. Q. Xu, *J. Phys. Chem. C* **2008**, 112, 15176–15182.
- [6] a) C. Xue, C. A. Mirkin, *Angew. Chem.* **2007**, 119, 2082–2084; *Angew. Chem. Int. Ed.* **2007**, 46, 2036–2038; b) J. A. Zhang, M. R. Langille, C. A. Mirkin, *J. Am. Chem. Soc.* **2010**, 132, 12502–12510.
- [7] D. M. Ledwith, A. M. Whelan, J. M. Kelly, *J. Mater. Chem.* **2007**, 17, 2459–2464.
- [8] a) G. S. Métraux, C. A. Mirkin, *Adv. Mater.* **2005**, 17, 412–415; b) I. Washio, Y. J. Xiong, Y. D. Yin, Y. N. Xia, *Adv. Mater.* **2006**, 18, 1745–1749.
- [9] N. Cathcart, A. J. Frank, V. Kitaev, *Chem. Commun.* **2009**, 7170–7172.
- [10] a) Q. Zhang, J. Ge, T. Pham, J. Goebel, Y. Hu, Z. Lu, Y. Yin, *Angew. Chem.* **2009**, 121, 3568–3571; *Angew. Chem. Int. Ed.* **2009**, 48, 3516–3519; b) J. An, B. Tang, X. H. Ning, J. Zhou, S. P. Xu, B. Zhao, W. Q. Xu, C. Corredor, J. R. Lombardi, *J. Phys. Chem. C* **2007**, 111, 18055–18059.
- [11] J. Zeng, X. H. Xia, M. Rycenga, P. Henneghan, Q. G. Li, Y. N. Xia, *Angew. Chem.* **2011**, 123, 258–263; *Angew. Chem. Int. Ed.* **2011**, 50, 244–249.
- [12] J. E. Millstone, S. J. Hurst, G. S. Metraux, J. I. Cutler, C. A. Mirkin, *Small* **2009**, 5, 646–664.
- [13] V. Germain, J. Li, D. Ingert, Z. L. Wang, M. P. Pileni, *J. Phys. Chem. B* **2003**, 107, 8717–8720.
- [14] D. Aherne, D. M. Ledwith, M. Gara, J. M. Kelly, *Adv. Funct. Mater.* **2008**, 18, 2005–2016.
- [15] a) J. L. Elechiguerra, J. Reyes-Gasca, M. J. Yacaman, *J. Mater. Chem.* **2006**, 16, 3906–3919; b) C. Lofton, W. Sigmund, *Adv. Funct. Mater.* **2005**, 15, 1197–1208.
- [16] Q. Zhang, N. Li, J. Goebel, Z. Lu, Y. Yin, *J. Am. Chem. Soc.* **2011**, 133, 18931–18939.
- [17] a) X. C. Jiang, Q. H. Zeng, A. B. Yu, *Langmuir* **2007**, 23, 2218–2223; b) B. Tang, J. An, X. L. Zheng, S. P. Xu, D. M. Li, J. Zhou, B. Zhao, W. Q. Xu, *J. Phys. Chem. C* **2008**, 112, 18361–18367.
- [18] B. Tang, S. P. Xu, J. An, B. Zhao, W. Q. Xu, *J. Phys. Chem. C* **2009**, 113, 7025–7030.
- [19] G. S. Métraux, Y. C. Cao, R. C. Jin, C. A. Mirkin, *Nano Lett.* **2003**, 3, 519–522.
- [20] C. Xue, J. E. Millstone, S. Y. Li, C. A. Mirkin, *Angew. Chem.* **2007**, 119, 8588–8591; *Angew. Chem. Int. Ed.* **2007**, 46, 8436–8439.